Z. Phys. B – Condensed Matter 71, 455–463 (1988)

Condensed
Zeitschrift für Physik B Matter

Variable-range hopping conduction in doped germanium at very low temperatures and high magnetic fields

W. Schoepe
Institut für Angewandte Physik, Universität Regensburg, Federal Republic of Germany

Received February 8, 1988

The conductivity of doped Ge below the metal–insulator transition is measured at temperatures between 4 K and 40 mK and in magnetic fields up to 7 Tesla. In zero field the resistivity exponent diverges as $T^{-1/2}$. In weak fields the magnetoresistance increases as B^2 and becomes exponentially large in strong fields and at low temperatures. The results can be described quantitatively in terms of variable-range hopping between localized states having a Coulomb gap in the density of states at the Fermi level. The magnetoresistance is calculated for arbitrary fields by means of a quasi-classical method. A fit to the data gives the radius of the localized states and the density of states. The sample is found to be very close to the metal-insulator transition. A small increase of the binding energy is observed in strong fields.

I. Introduction

At very low temperatures the electrical conductivity of doped semiconductors depends upon the density of states close to the Fermi energy and on the radius of localization of the charge carriers bound to impurity states ("Bohr radius"). At very high doping levels the large overlap of the wavefunctions leads to an impurity-band conduction and results in a finite conductivity at $T=0$: the system has become metallic. Below the metal–insulator transition, however, the carriers are localized and charge transport takes place by hopping conduction. At sufficiently low temperatures, i.e. when the thermal energy kT is much smaller than the energy difference between adjacent localized states, hopping becomes increasingly slow and the resistance diverges at $T=0$. In this regime the localized wavefunction has to sample an increasingly larger volume to find a state whose energy is close enough to be accessible. Charge transport now is a tunneling process including thermal activation being supplied by the phonons. This mechanism is known as "variable-range hopping" (VRH) and there is an extensive literature on this subject [1]. Assuming a constant density of states g at the Fermi level and an exponential decay of the wavefunction $\exp-(2r/a_0)$ where a_0 is the Bohr radius and r the distance, the resistance R is calculated to diverge according to Mott's law

$$R(T)=R_0\exp(T_0/T)^{1/4}, \tag{1}$$

with $T_0 \propto (ga_0^3)^{-1}$. This has been observed in various systems. On the other hand, there are experiments which indicate a somewhat different divergence, namely

$$R(T)=R_0\exp(T_0/T)^{1/2}. \tag{2}$$

This has been discussed by Efros and Shklovskii [1] as a result of a density of states (DOS) which vanishes quadratically at the Fermi level because of the Coulomb interaction between initial and final hopping sites. In fact, for large hopping lengths the Coulomb interaction dominates the energy difference between the sites. Therefore, the $T^{-1/2}$-law (2) will replace Mott's $T^{-1/4}$-law (1) at very low temperatures with a transition temperature which decreases for higher doping levels. The quantity T_0 in (2) is determined by $(\varepsilon a_0)^{-1}$, where ε is the dielectric constant of the semiconductor.

Considerably more detailed information on VRH conduction can be obtained by applying a magnetic field in addition to varying the temperature of the

sample because the field alters the wavefunction. The exponential tail of the wavefunction is contracted and thus the probability of a hop is reduced. This leads to a large positive magnetoresistance (MR) having a strong temperature dependence which is characteristic of the particular DOS [1]. From measurements of the MR in weak fields and from T_0 being measured in zero field the Bohr radius and the DOS can be determined separately. Experiments on the MR in the VRH regime have been performed with *n*-Ge [2, 3], *n*-InP [4, 5], *n*-InSb [6, 7], doped polyacetylene [8, 9] and polypyrrole [10]. In large fields B, when the cyclotron radius $\lambda = (\hbar/eB)^{1/2}$ becomes smaller than the Bohr radius a_0, the MR is predicted to have field and temperature dependences which are different from the weak field limit $\lambda \gg a_0$. This regime has been studied in *n*-InSb [7]. These results have stimulated further theoretical work [11, 12] which has not yet been tested experimentally. In particular, there seem to be no data for intermediate fields $\lambda \approx a_0$, a regime which is difficult to describe theoretically. Other open questions concern, e.g., the anisotropy of VRH with respect to a strong field or the influence of the metal–insulator transition which causes both the Bohr radius and the dielectric constant to become large.

Because the problem of how a doped semiconductor below the metal–insulator transition ceases to conduct as the temperature goes to zero is of fundamental importance, it seems desirable to obtain further experimental information for a better understanding of the VRH conduction. The present work describes an investigation of doped germanium at temperatures below 4 K and in magnetic fields up to 7 Tesla. The $T^{-1/2}$-law (2) is found to apply below 1.5 K down to the lowest temperature where the resistance has increased by six orders of magnitude. The data cover a sufficiently wide range of temperatures and fields to permit a detailed analysis. It turns out that the essential features of the experimental results are in quantitative agreement with theory.

This article is organized as follows. Chapter II describes experimental details, the results are presented in Chap. III. Based on the theory which is outlined in Chap. IV, the data are discussed in Chap. V. A final resumè is given in VI. The Appendix contains some further theoretical considerations.

II. Experimental details

The sample is a commerically available germanium thermometer [13]. No information on the composition or the concentration of the impurities could be obtained from the supplier. It seems likely, however, that the sample is made of As-doped *n*-Ge. It has been used for thermometry down to 0.3 K for more than 10 years and found to be quite reproducible. The reason for extending its use to lower temperatures is the simple temperature dependence (2) below 1 K which makes resistance thermometry at dilution refrigerator temperatures more easy [14]. Another advantage of the sample lies in the fact that it allows four-terminal measurements and therefore contact resistances between the leads and the sample area do not affect the data. This is of particular importance at very low temperatures and at high magnetic fields. So far, most of the published work seems to have been made with two-terminal samples.

Above 0.3 K the resistance was measured with an ac bridge while at lower temperatures the voltage between the potential leads was detected directly by an ac voltmeter having a high-impedance differential input. The measuring current was reduced from 1 μA to 0.1 nA as the temperature was lowered to avoid heating effects. Also the frequency had to be reduced to 1 Hz at the lowest temperatures in order to prevent the rf filters of the current and voltage leads from shortening out the high-ohmic sample.

Initially the temperature was recorded by a second germanium thermometer which had been calibrated against a ^{3}He melting curve thermometer [15]. For thermometry in a magnetic field a carbon resistor was used [16] which also followed (2) but which had only a very small MR [17, 18]. Both the sample and the thermometers were mounted inside the mixing chamber of a dilution refrigerator. Data above 0.3 K had been taken earlier in a ^{3}He cryostat.

In MR measurements one may have to take into account (or eliminate) geometry dependent Hall voltages. In the VRH regime, though, the Hall effect is known to be extremely small – if it exists at all. By reversing the direction of the field no measurable Hall voltages were found to be superimposed upon the signal.

The data to be presented in the following chapter were taken either by varying the temperature of the sample in a fixed field or (less conveniently) by stabilizing the temperature and sweeping the field.

III. Results

The temperature dependence of the resistance is depicted in Fig. 1. From the straight-line behavior it is obvious that the data can be described by (2) whereas Mott's law (1) does not apply. In zero field one finds $T_0 = 11.1$ K. Also in the fields a straight line can be fit to the data. However, as will be shown later, a slightly different temperature dependence, viz. $T^{-0.6}$ instead

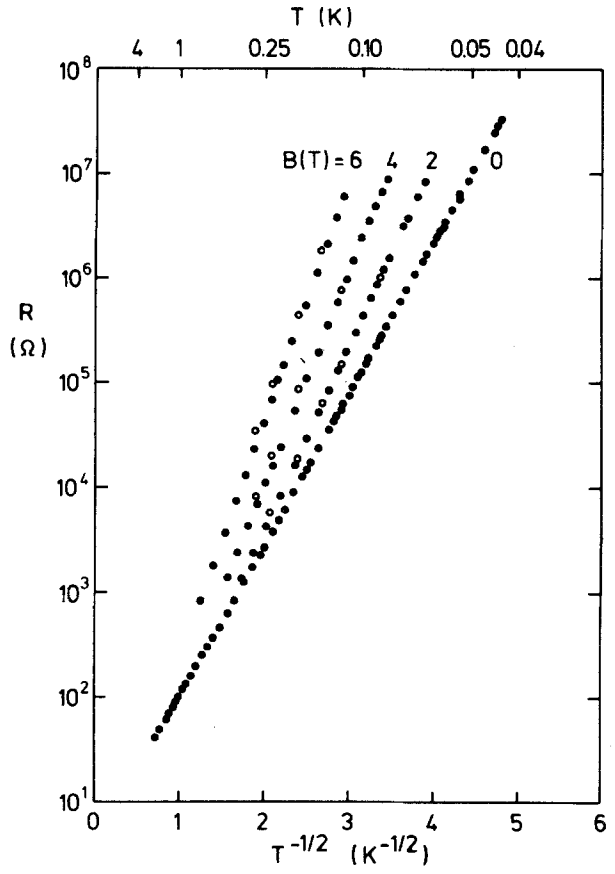

Fig. 1. Temperature dependence of the resistance. The data for $B \neq 0$ were obtained either with the field parallel to the current (dots) or perpendicular (circles)

of $T^{-0.5}$, fits equally well and yields slopes which can be understood quantitatively.

These results were obtained with the field parallel to the encapsulated sample, i.e. parallel to the current. In principle, an anisotropy should be expected in high fields [1]. In subsequent runs (see below) the orientation of the capsule was changed to be perpendicular to the field. Surprisingly little anisotropy was found.

To study the weak field behavior the temperature was kept stable while the field was swept slowly. The relative change $\Delta R/R(0)$ is shown in Fig. 2, where $\Delta R \equiv R(B) - R(0)$. At all temperatures the MR starts to grow as B^2:

$$\Delta R/R(0) = B^2/B_0^2. \tag{3}$$

The coefficient B_0^2 is strongly temperature dependent, see Fig. 3. Below 0.5 K it follows a power law T^m, with $m = 1.6 \pm 0.1$. Towards higher temperatures B_0^2 grows more slowly. At 4.2 K the quadratic increase extends up to at least 3 Tesla while towards lower temperatures this regime shrinks considerably.

In Fig. 4 the large-field MR $R(B)/R(0)$ is plotted at various fixed temperatures. It is obvious that the MR

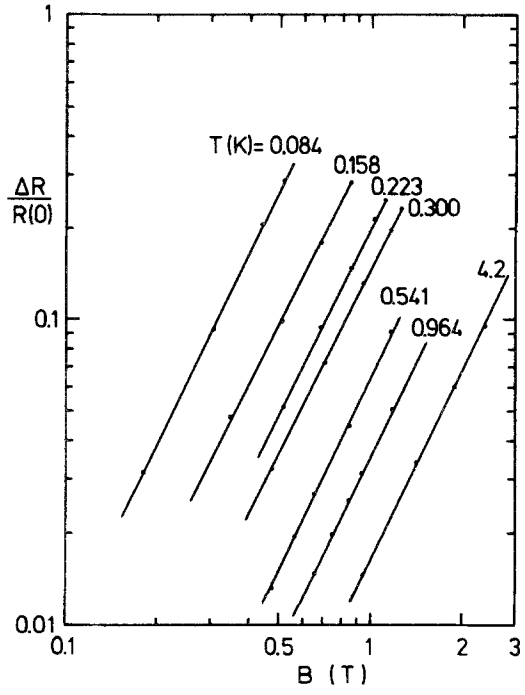

Fig. 2. Magnetoresistance in weak fields. The slopes are 2 ± 0.1 indicating a B^2 dependence

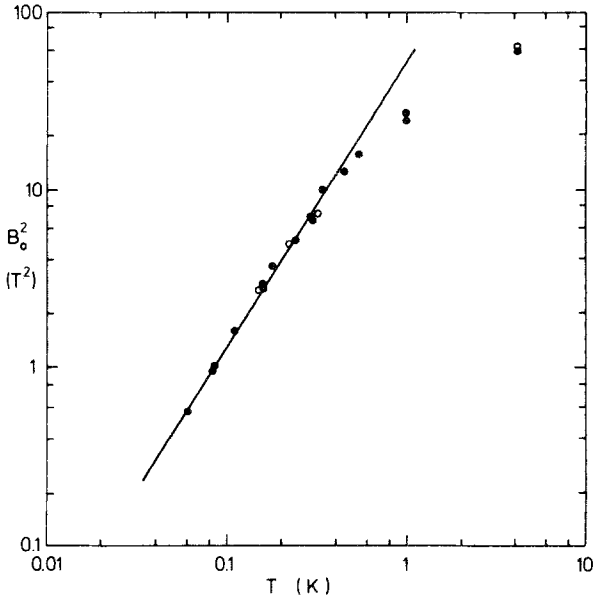

Fig. 3. The coefficient B_0^2 of the weak field magnetoresistance of Fig. 2. Open circles: field parallel to current, dots: perpendicular orientation. The slope of the straight line is 1.58 ± 0.1 in agreement with $B_0^2 \propto T^{3/2}$

becomes exponentially large. At the lower temperatures the sample soon became so high-ohmic that it could not be measured reliably with the present method. (Usually the sweep was terminated when the

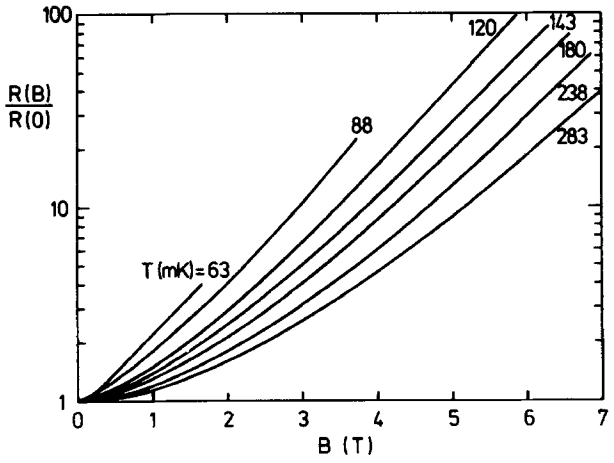

Fig. 4. Magnetoresistance as a function of the field at various constant temperatures (transverse geometry)

sample had reached several MΩ. Also because of the steep temperature dependence of the MR temperature stability became increasingly critical.)

The data in Fig. 4 were obtained with the field perpendicular to the capsule (i.e. to the current) in contrast to those of Fig. 1. Comparison of the values at 2 and 4 Tesla, respectively, gives good agreement whereas at 6 Tesla they are slightly higher (see Fig. 1). This could be a sign of the expected anisotropy mentioned above. Because of the rather small size of the effect, however, this was not investigated in more detail.

IV. Theory

By means of percolation theory the exponential dependences on temperature and magnetic field of VRH conduction can be calculated easily in the limits of weak and strong fields [1]. Let ΔE_ξ be an energy interval around the Fermi energy whose extension depends on the percolation parameter ξ, and V_ξ the corresponding volume around a site, then the number of sites $n(\xi)$ within V_ξ for a DOS dN/dE is given by

$$n(\xi) = \int_{V_\xi} dV \int_{\Delta E_\xi} \frac{dN}{dE} dE. \tag{4}$$

The problem consists of finding a lower bound ξ_c of ξ and the critical number $n_c = n(\xi_c)$ for percolation to occur for the appropriate dependences ΔE_ξ and V_ξ. The resistance is then given by

$$R = R_0 \cdot \exp(\xi_c). \tag{5}$$

For an isotropic wavefunction having an exponential decay the bonding criterion

$$2r/a_0 + \Delta E/kT \leq \xi$$

gives $\Delta E_\xi = kT\xi$ and $V_\xi = 4\pi r_\xi^3/3 = 4\pi(\frac{a_0}{2}\xi)^3/3$. Assuming a quadratic DOS at the Fermi energy E_F, viz.:

$$dN/dE = g_0 \Delta E^2,$$

where $\Delta E = E - E_F$, one finds from (4)

$$n_c = 2 \cdot \frac{1}{3} g_0 (kT\xi_c)^3 \cdot \frac{4}{3}\pi \left(\frac{a_0}{2}\xi_c\right)^3. \tag{6}$$

Hence

$$\xi_c = (T_0/T)^{1/2} \tag{7}$$

with $T_0 = (9n_c/\pi g_0 a_0^3 k^3)^{1/3}$. The number n_c has been calculated numerically, see [1]. Inserting (7) into (5) gives (2). For a Coulomb gap g_0 is proportional to ε^3, where ε is the dielectric constant of the semiconductor, which implies $T_0 = \beta e^2/4\pi\varepsilon_0 \varepsilon a_0 k$, where $\beta \approx 2.8$ is a numerical factor [19].

The calculation of the field dependence [1] can be summarized as follows. In a weak field the wavefunction decays faster at long distances due to the B^2 potential perpendicular to the field axis, viz.: $r^3 a_0 \sin^2\theta/12\lambda^4$, where θ is the angle of r with respect to the field. By inserting the zero-field result $r_\xi = a_0\xi/2$ one finds a small correction $\Delta\xi_c(B)$ for the resistivity exponent, viz.:

$$\Delta\xi_c(B) \equiv \xi_c(B) - \xi_c(0) = \ln(R(B))/R(0)) = B^2/B_0^2, \tag{8}$$

where $B_0^2 = (\alpha\hbar^2/e^2 a_0^4)\ (T/T_0)^{3/2}$ and $\alpha \approx 6.6 \cdot 10^2$ is a numerical factor [19].

In a very strong field ($\lambda \ll a_0$) the wavefunction becomes highly anisotropic. Perpendicular to the field the length scale is now set by λ, whereas along the field axis it will not change very much. V_ξ and ΔE_ξ are determined from the condition

$$2|z|/a_B + (x^2 + y^2)/2\lambda^2 + \Delta E/kT \leq \xi$$

where the z-axis is chosen along the field. The shape of V_ξ has changed from a sphere to a double paraboloid of a volume $V_\xi = \pi a_B \lambda^2 \xi^2$. Instead of (6) and (7) one finds now

$$n_c = 2 \cdot \frac{1}{3} g_B (kT\xi_c)^3 \cdot \pi a_B \lambda^2 \xi_c^2 \tag{9}$$

and therefore

$$\xi_c(B) = (T_1(B)/T)^{3/5} \text{ with}$$

$$T_1(B) = T_0 \cdot \left(\frac{e a_0^2 B}{6\hbar} \cdot \frac{a_0}{a_B} \cdot \frac{g_0}{g_B}\right)^{1/3}. \tag{10}$$

The factor g_B in the DOS and the length a_B may depend on the field while n_c is assumed to be independent of the shape of V_ξ [19].

For intermediate fields the wavefunction of a shallow donor is extremely complicated and the overlap integral cannot be obtained analytically. For this

reason the MR has not yet been calculated in this regime. Because most of the data of the present work fall into this regime it is necessary to look for an alternative solution of the problem. A similar situation exists in the case of nearest-neighbor hopping. There the MR has been calculated by Ioselevich [20] for arbitrary fields by employing the quasi-classical method. The overlap integral was shown to be given by the action integral taken along an electron path between initial and final site. For bound states the motion of the electron is imaginary but the action integral is real and positive. Having obtained the overlap integral he could calculate the volume V_ξ for arbitrary fields. In the following I make use of his result and extend it to the case of VRH.

With E_0 being the binding energy of the localized state, m the effective mass of the electron, and $\omega = eB/m$ the cyclotron frequency, Ioselevich's result for V_ξ is [20]:

$$V_\xi = 8\pi\left(\frac{2|E_0|}{m\omega^2}\right)^{3/2} F\left(\frac{\xi\hbar\omega}{4|E_0|}\right), \tag{11}$$

where

$$F(s) = \int_{\tau(s)}^{s}\left[th\left(\frac{x}{2}\right)\cdot(shx + x - 2s) + (s-x)x\right] \times \frac{(shx + x - 2s)^{1/2}\cdot x\cdot shx}{(shx - x)^{5/2}}\,dx,$$

with $\tau(s)$ being the solution of

$$sh\tau + \tau - 2s = 0.$$

Equation (11) describes the gradual change of V_ξ from the sphere to the double paraboloid as the field grows.

$\xi_c(B)$ can now be determined. It is convenient to introduce the reduced variables

$$\xi^* \equiv \xi_c(B)/\xi_c(0)$$

and

$$B^* \equiv B/B_c,$$

with B_c being defined by

$$B_c \equiv 6\hbar/ea_0^2\xi_c(0).$$

Calculating n_c and dividing the result by (6) yields the following relation between ξ^* and B^*:

$$F(3B^*\xi^*) = \frac{9}{2}\cdot\frac{g_0}{g_B}\cdot\left(\frac{B^*}{\xi^*}\right)^3. \tag{12}$$

If the binding energy in a field E_B is the different from the zero field value $E_0 = \hbar^2/2ma_0^2$, I find that (12) assumes the more general form

$$F\left(3B^*\xi^*\frac{E_0}{E_B}\right) = \frac{9}{2}\cdot\frac{g_0}{g_B}\cdot\left(\frac{B^*}{\xi^*}\sqrt{\frac{E_0}{E_B}}\right)^3. \tag{13}$$

From (13) the MR is determined if the field dependences of g_B and E_B are known. For a Coulomb gap one has $g_0/g_B = (\varepsilon(0)/\varepsilon(B))^3$.

In order to compare the general solution (13) with the earlier results for weak and strong fields, i.e. (8) and (10), I use the following analytical approximations for F:

$$F(s) \approx \frac{s^3}{6} - \frac{s^5}{72} \qquad \text{for} \quad s \le 1, \tag{14}$$

and

$$F(s) \approx \frac{s^2}{2} \qquad \text{for} \quad s \ge 10. \tag{15}$$

For $B^* \ll 1$, $E_B = E_0$, and $g_B = g_0$ I find from (13) and (14)

$$\xi^* = 1 + \frac{1}{8}B^{*2}, \tag{16}$$

which gives the known weak field result (8) with a numerical factor $\alpha = 288$ instead of $\simeq 660$.

For strong fields one readily obtains (10) from (13), (15), and (7) by using $(E_B/E_0)^{1/2} = a_0/a_B$. Thus, the general solution (13) reproduces the known asymptotic limits.

The function $\xi^*(B^*)$ calculated from (13) for the simplified case of $E_B = E_0$ and $g_B = g_0$ is depicted in Fig. 5. Note the gradual transition from the initial rise as B^{*2} (16) to the final $B^{*1/5}$-behavior (10).

So far, it was always assumed that the wavefunction is isotropic in zero field. This, of course, is not the case in germanium where V_ξ consists of four rotational ellipsoids whose axes are oriented along the four triad axes of a cube. The anisotropy has been discussed in detail for the case of nearest-neighbor hopping [1, 21]. From symmetry considerations it was shown that in the weak field limit, where the MR

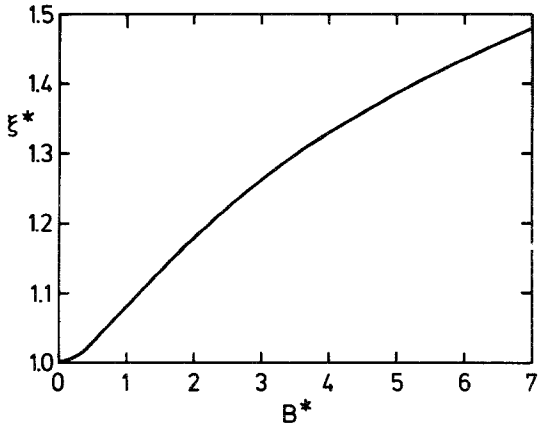

Fig. 5. Reduced resistivity exponent ξ^* vs. reduced field B^* as calculated from (13) for the case of $E_B = E_0$ and $g_B = g_0$

depends on B^2, no anisotropy is to be expected. In strong fields, however, an anisotropy of the MR has been observed [22] and described [21]. In the VRH regime one may expect the situation to be similar. The ellipsoid whose axis of revolution is closest to the direction of the field will be compressed the most whereas the one which is rather perpendicular to field will be affected less (the ratio of the transverse and longitudinal Bohr radii is 4.5). The shape of V_ξ then becomes exceedingly complicated. Employing the quasi-classical method, therefore, appears to be a prohibitively difficult task and the small anisotropy seen in this work is rather discouraging. The solution of the simplified problem of one ellipsoid being oriented along the field is given in the Appendix.

Finally, it should be mentioned that a completely different structure of the wavefunction in a high magnetic field has recently been proposed by Shklovskii [11, 12]. In that work it is suggested that the tunneling electron is scattered along its path. The result is that the magnetic potential barrier does not grow with increasing distance from the donor but rather assumes a constant value. This theory leads to a $T^{-1/2}$-law (2) also for intermediate and strong fields with a field dependence of T_0, viz.:

$$T_0(B) = T_0(0) \cdot (1 - f(B))^{-2/3}, \tag{17}$$

where $f(B)$ is calculated to change from a $B^{2/3}$ dependence to $B^{6/5}$ for intermediate fields, and in strong fields (17) should go over to

$$T_0(B) \propto B^{1/2}. \tag{18}$$

Close to the metal–insulator transition the variation of $f(B)$ in (17) is predicted to be slightly altered [12] while (18) will remain valid. The weak field result (8) should not be affected by the subbarrier scattering.

V. Discussion

From $T_0 = 11.1$ K and B_0^2 the localization radius a_0 and the dielectric constant ε can be determined. Below 0.5 K B_0^2 is in agreement with the $T^{3/2}$ dependence of (8) and (16). For $\alpha = 288$ as obtained from (16) the data in Fig. 3 yield $a_0 = 170$ Å. Inserting this value into $T_0 = 2.8\, e^2/4\pi\varepsilon_0\varepsilon a_0 k$ gives $\varepsilon = 248$. Both values are greatly enhanced due to the proximity of the metal–insulator transition. Taking a dielectric constant of 16 and an effective Bohr radius of 40 Å far away from the transition the above values indicate an enhancement of ε by a factor of 16 and of a_0 by a factor of 4. This agrees with predictions from scaling theory, viz.:

$$a_0(N) = a_0(0)(1 - N/N_c)^{-\nu}$$

and

$$\varepsilon(N) = \varepsilon(0)(1 - N/N_c)^{-\zeta},$$

which gives

$$\varepsilon(N)/\varepsilon(0) = (a_0(N)/a_0(0))^{\zeta/\nu}. \tag{19}$$

Experiments on the metal–insulator transition in other systems indicate [23] $\nu \simeq 1/2$ and $\zeta \simeq 1$, thus $\zeta/\nu \simeq 2$. From these results one finds $(1 - N/N_c) = 6.5 \cdot 10^{-2}$ for the present case: the doping level N is very close to the transition at N_c. In [3] only slightly different values of a_0 and ε at $T_0 \simeq 10$ K were obtained from MR measurements on doped Ge at higher temperatures because these authors used $\alpha \simeq 660$ in (8) for their analysis.

The deviation of B_0^2 from the $T^{3/2}$ dependence above 0.5 K signals the disappearance of the Coulomb gap. (In the regime of Mott's law (1) B_0^2 should increase as $T^{3/4}$ and for nearest-neighbor hopping it will become temperature independent.) It is interesting to note that the deviation is seen clearly in the MR data of Fig. 3 whereas in zero field no deviation from $T^{-1/2}$-law is detectable in Fig. 1 up to 1.5 K even if one expands the scales considerably. The MR is more sensitive to changes in $\xi_c(0)$ than the temperature dependence of R in zero field because $B_0^2 \propto \xi_c(0)^{-3}$, see (8). The width δ of the Coulomb gap can now be estimated by comparing it with the available energy range ΔE_{ξ_c} at 0.5 K:

$$\delta/k \simeq \Delta E_{\xi_c}/k = T\xi_c = (T_0 T)^{1/2} = 2.4 \text{ K}. \tag{20}$$

Analyzing the MR in large fields one might conclude that the apparent $T^{-1/2}$-behavior in Fig. 1 seems to be in conflict with the $T^{-3/5}$-law (10). Alternatively, applying the result of Shklovskii's subbarrier scattering theory (17) gives the correct temperature dependence but not the observed field dependence $T_0(B)$ when the slopes in Fig. 1 are evaluated (which turn out to depend linearly on B). The apparent contradiction with (10) is resolved when plotting the temperature dependence of the sample in the field *vs.* $T^{-3/5}$, see Fig. 6. Again a straight line dependence is obtained [24]. However, comparing the slopes $T_1(B)$ with (10) gives good agreement. From Fig. 6 one finds $T_1(2T) = 5.6$ K, $T_1(4T) = 7.2$ K, and $T_1(6T) = 9.4$ K [24]. Using $a_0 = 170$ Å and assuming $a_0 = a_B$ and $g_0 = g_B$, (10) yields 5.9 K, 7.4 K, and 8.4 K, respectively. The slight difference at $B = 6T$ may be attributed to a decrease of a_B. Assuming that the dielectric constant scales as a_B^2 (like in zero field, see (19)) gives an estimate of g_0/g_B, viz.:

$$g_0/g_B = (\varepsilon(0)/\varepsilon(B))^3 \simeq (a_0/a_B)^6. \tag{21}$$

With $T_0 = 11.1$ K and $T_1(6T) = 9.4$ K one has from (10) and (21) $a_0/a_B = 1.05$ at 6 Tesla.

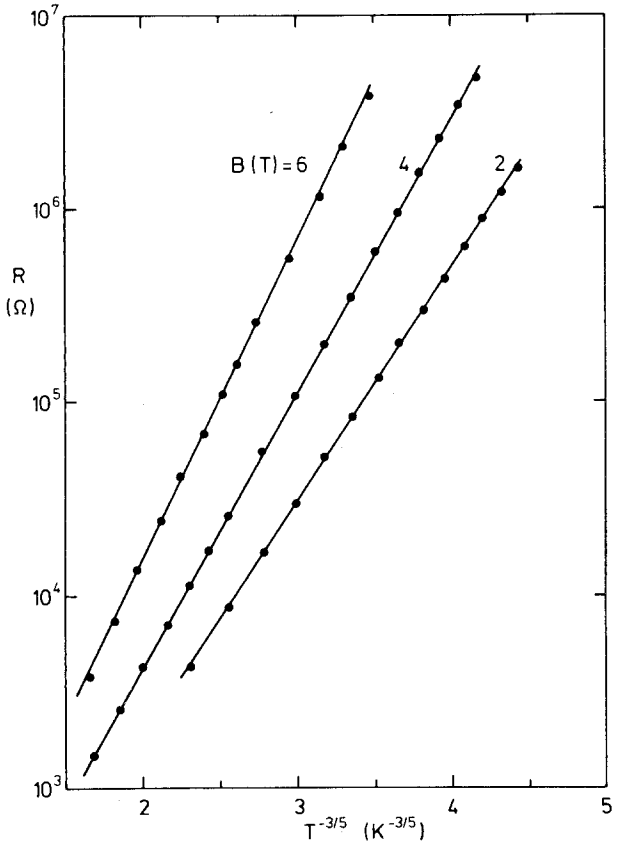

Fig. 6. Temperature dependence of the resistance in large fields vs. $T^{-3/5}$ (same data as in Fig. 1)

In order to compare the data of Fig. 4 with theory one has to apply the general solution (13) because now the field covers the entire range from weak to strong. With the assumption (21) and by substituting a_0/a_B by $(E_B/E_0)^{1/2}$, (13) reduces to

$$F(3B^*\xi^*E_0/E_B) = \frac{9}{2}(B^*/\xi^*)^3(E_B/E_0)^{3/2}. \tag{22}$$

Now, (22) can be solved for E_B/E_0 at a given data point (ξ^*, B^*) which can be calculated from T_0 and a_0. The result is shown in Fig. 7. One should, of course, expect the ratio E_B/E_0 to be a function of the field only and not to depend on temperature. The reason why the ratio grows at large fields and high temperatures is due to the finite width δ of the Coulomb gap: at 6 Tesla the data at 0.283 K and 0.238 K imply a $\Delta E_{\xi_c}/k = 2.6$ K and 2.4 K, respectively, and thus violate the requirement $\Delta E_\xi \ll \delta$ for a Coulomb gap to be completely developed (see (20)). From $\xi_c(B)$ given by (10) this condition can be written in general form as

$$T \ll (\delta/k)^{5/2} \cdot T_1(B)^{-3/2}. \tag{23}$$

In a field of 6 Tesla this means $T \ll 0.3$ K. Therefore, (13) is not strictly valid at 0.283 K and 0.238 K. It is simple to calculate the MR for a constant density of

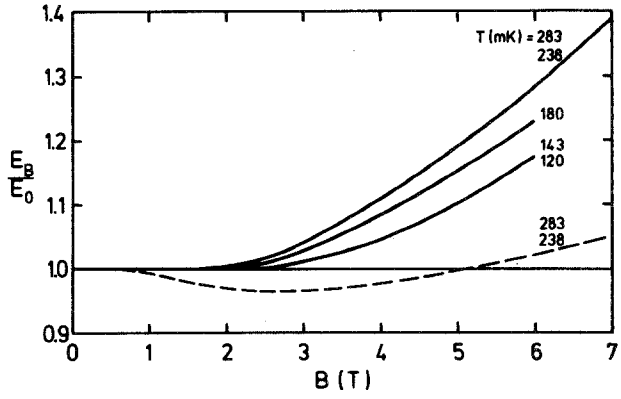

Fig. 7. The function E_B/E_0 obtained by solving (22) for the data of Fig. 4. The dashed curve is the solution of (A1) which is calculated for a constant density of states at the Fermi level

states by means of the quasi-classical method (see (A1) in the Appendix) and then to solve for E_B/E_0. If this is done for the two highest temperatures in Fig. 4 one finds $E_B/E_0 = 1.05$ at $B = 6$ T.

At the lowest temperatures the Coulomb gap does not vanish even at 6 Tesla. The data of Fig. 4 taken at 0.143 K and 0.120 K actually do give the same result for E_B/E_0. An interpretation of the observed field dependence, however, cannot be offered at present. Also, to my knowledge, there are no other experiments on the field dependence of the binding energy of a shallow donor in Ge close to the metal–insulator transition with which the present data could be compared [25]. Finally, one should keep in mind the various assumptions and approximations which have been made in obtaining (22). In particular, if different numerical factors are used in the above analysis the resulting E_B/E_0 will be somewhat different [19]. In addition, one cannot rule out any influence by a possible field dependence of the pre-exponential factor R_0, which so far has been neglected completely.

VI. Summary

The experimental results of the temperature and field dependences of the conductivity can be described quantitatively and consistently in terms of VRH conduction with a Coulomb gap in the DOS at the Fermi level. From the data in weak fields the localization radius and the dielectric constant are deduced. Both are largely enhanced because of the proximity of the metal–insulator transition. The data obtained in strong fields indicate a small field dependence of the binding energy of the localized state. A quasi-classical calculation permits an analysis of the MR at arbitrary fields. Subbarrier scattering of the tunneling electron is not relevant in the present case.

The small anisotropy of the conductivity with respect to the direction of the field is rather surprising. Future experiments on samples whose orientation can be controlled more systematically appear necessary to investigate this problem in detail.

Finally, it is interesting to note that the carbon resistor used here for thermometry also obeys the $T^{-1/2}$-law (2) while its MR is completely different from that of the Ge sample, namely very small (few percent) and negative. Clearly, the details of charge transport in these systems are quite different in spite of the common $T^{-1/2}$-behavior in zero field.

I am most grateful to K. Neumaier for the detailed advice on how to build a dilution refrigerator which cools to 11 mK with just a continuous heat exchanger. K. Uhlig kindly calibrated the germanium resistor against his ^{3}He melting curve thermometer and also gave numerous and valuable cryogenic advice. Thanks are due to E. Ettlinger and K. Lachner for the construction of the refrigerator. W. Prettl, G. Jungwirt, and M. Weispfenning patiently answered all the questions I had about the physics of shallow donors. Support and encouragement by K.F. Renk is gratefully acknowledged. This work was financially supported by a grant of the Volkswagen Foundation.

Appendix

1. Numerical factors

The quantitative analysis of the data in this work requires three numerical factors which are not known with good precision. One is β in T_0 in (7), another one is α in B_0^2, see (8), and the third one is in $T_1(B)$ in (10). The value of α affects the Bohr radius a_0, β then determines the dielectric constant ε, and the factor 6 in (10) the binding energy E_B/E_0. Detailed considerations [1] indicate $\beta \simeq 2.8$ and this value is adopted here. The factors in B_0^2 and $T_1(B)$ used in this work result from the quasi-classical calculation and are based on the assumption that n_c is independent of the shape of V_ξ, which may be questioned. Furthermore, in calculating n_c the double integral (4) is replaced by the product of a volume and an energy integral. Performing the exact integration yields only a numerical factor in (6) and (9) which, however, depends on the shape of V_ξ. The result would be a change of E_B/E_0 in large fields by a factor of $4^{1/7} = 1.22$. With the data of this work being sufficiently detailed for a quantitative analysis a more precise knowledge of the numerical factors is desirable.

2. Constant DOS

The quasi-classical method is used to calculate the MR at arbitrary fields in case of a constant DOS at the fermi level $dN/dE = g$. For $B = 0$ one has

$$n_c = 2gkT\xi_c(0) \cdot \frac{4}{3}\pi\left(\frac{a_0}{2}\xi_c(0)\right)^3,$$

and in a finite field

$$n_c = 2gkT\xi_c(B) \cdot V_\xi,$$

where V_ξ is Ioselevich's result (11). Repeating the same steps as in Chap. IV gives instead of (13):

$$F(3B^*\xi^* E_0/E_B) = (9B^{*3}/2\xi^*)(E_0/E_B)^{3/2}. \qquad \text{(A1)}$$

The asymptotic limits of (A1) reproduce the known results [1]:

$\xi_c(B) - \xi_c(0) \propto B^2/T^{3/4}$ in weak fields,

and

$\xi_c(B) \propto (B/T)^{1/3}$ in strong fields.

3. Anisotropic wavefunction

For an anisotropic wavefunction the MR can be calculated most easily for the case when the field is oriented along the axis of revolution of the ellipsoid. Let $\mu = \dfrac{m_l}{m_t} = \left(\dfrac{a_t}{a_l}\right)^2$ be the ratio of the effective masses along and transverse to the direction of the field (for Ge: $\mu \approx 20$) and $\omega_t = eB/m_t$ the transverse cyclotron frequency. The quasi-classical method gives then

$$V_\xi = 8\pi\left(\frac{2|E_0|}{m_t\omega_t^2\mu^{1/3}}\right)^{3/2} \cdot F\left(\frac{\xi\hbar\omega_t}{4|E_0|}\right),$$

while in zero field $V_\xi = 4\pi a_t^2 a_l \xi(0)^3/24$. The MR is determined again by (12) with the characteristic field being defined by $B_c \equiv 6\hbar/ea_t^2\xi_c(0)$. For arbitrary orientation of the ellipsoid with respect to the field the calculation becomes considerably more complicated.

References

1. For an excellent recent review see Shklovskii, B.I., Efros, A.L.: Electronic properties of doped semiconductors. Berlin, Heidelberg, New York: Springer 1984
2. Shlimak, I.S., Ionov, A.N., Shklovskii, B.I.: Fiz. Tekh. Poluprov. **17**, 503 (1983) [English transl.: Sov. Phys.–Semicond. **17**, 314 (1983)]
3. Ionov, A.N., Shlimak, I.S., Matveev, M.N.: Solid State Commun. **47**, 763 (1983)
4. Abboudy, S., Mansfield, R., Fozooni, P.: High magnetic fields in semiconductor physics. Landwehr, G. (ed.), pp. 518. Berlin, Heidelberg, New York: Springer 1987
5. Biskupski, G., Dubois, H., Laborde, O.: Application of high magnetic fields in semiconductor physics. Landwehr, G. (ed.). Berlin, Heidelberg, New York: Springer 1983

6. Gershenzon, E.M., Il'in, V.A., Litvak-Gorskaya, L.B.: Fiz. Tekh. Poluprov. **8**, 295 (1974) [English transl.: Sov. Phys. – Semicond. **8**, 189 (1974)]
7. Tokumoto, H., Mansfield, R., Lea, M.J.: Phil. Mag. B **46**, 93 (1982)
8. Ettlinger, E., Schoepe, W., Monkenbusch, M., Wieners, G.: Solid State Commun. **49**, 107 (1984)
9. Ettlinger, E., Ose, W., Schoepe, W.: Mol. Cryst. Liq. Cryst. **117**, 173 (1985)
10. Kücher, A.: Diploma thesis, Universität Regensburg 1986: (unpublished)
11. Shklovskii, B.I.: Zh. Eksp. Theor. Fiz. Pis. Red. **36**, 43 (1982) [English transl.: Sov. Phys. – JETP Lett. **36**, 51 (1982)
12. Shklovskii, B.I.: Fiz. Tekh. Poluprov. **17**, 2055 (1983) [English transl.: Sov. Phys. – Semicond. **17**, 1311 (1983)]
13. Scientific Instruments, Inc., 1101 25th Street, West Palm Beach, Fla. 33407, USA: model 4S-^{3}He
14. Schoepe, W., Uhlig, K.: (to be published)
15. The calibration was performed by K. Uhlig at the Walther-Meissner Institute, Garching
16. Thanks are due to K. Neumaier and P. Gutsmiedl at the Walther-Meissner Institute, Garching, for the loan of the carbon resistor
17. Lerbet, F., Bellessa, G.: Cryogenics **26**, 694 (1986)
18. Koike, Y., Fukase, T., Morita, S., Okamura, M., Mikoshiba, N.: Cryogenics **25**, 499 (1985)
19. For a discussion of the numerical factors see Appendix 1
20. Ioselevich, A.S.: Fiz. Tekh. Poluprov. **15**, 2373 (1981) [English transl.: Sov. Phys. – Semicond. **15**, 1378 (1981)]
21. Shklovskii, B.I., Nguen Van Lien: Fiz. Tekh. Poluprov. **12**, 1346 (1978) [English transl.: Sov. Phys. – Semicond. **12**, 796 (1978)]
22. Chroboczek, J.A., Sladek, R.J.: Phys. Rev. **151**, 595 (1966)
23. Rosenbaum, T.F., Milligan, R.F., Paalanen, M.A., Thomas, G.A., Bhatt, R.N.: Phys. Rev. B **27**, 7509 (1983)
24. Towards higher temperatures the data in Fig. 6 actually leave the strong field limit, though this is not visible in the figure
25. The binding energy of a single donor in a magnetic field is discussed in [1] and the references cited therein; for a detailed calculation see, e.g., Larsen, D.M.: J. Phys. Chem. Solids **29**, 271 (1968)

W. Schoepe
Institut für Angewandte Physik
Universität Regensburg
Universitätsstrasse 31
D-8400 Regensburg
Federal Republic of Germany